cces
Leading in Education, Research and Decision Support
Competence Center Environment and Sustainability
COGEAR: COupled seismogenic GEohazards in Alpine Regions

COGEAR

MODULE 1:

Validate the building inventory and important infrastructure in the test area
Del. No.: 1c.1.1
&
Development of theoretical fragility functions
Del. No.: 1c.1.2

Authors: Michel, C., Oropeza, M., and Lestuzzi, P.

Applied Computing and Mechanics Laboratory, EPFL

January 27, 2010

APPLIED COMPUTING AND MECHANICS LABORATORY
EPFL-ENAC-IIC-IMAC
Station 18 CH-1015 Lausanne
Switzerland

ÉCOLE POLYTECHNIQUE
FÉDÉRALE DE LAUSANNE

COGEAR PROJECT
Module 1c

Vulnerability and Risk

Clotaire MICHEL, Marcelo OROPEZA, Pierino LESTUZZI

2010

Abstract

This report summarizes the results of the vulnerability assessment in the framework of the COGEAR project (Module 1c) dedicated to the city of Visp (Valais, Switzerland). The characteristics of the building stock were first collected and a database was designed to store and analyze these data. Second, data on 21 typical buildings in Switzerland, including ambient vibration tests, and analytical models were computed in order to better understand the vulnerability of different buildings classes. Fragility curves for unreinforced masonry structures with rigid slabs are proposed according to a newly developed method. The issues concerning other building classes are also discussed. Combined with hazard computations performed in the other tasks of the project, the results of this work will allow to develop risk and scenario maps with the corresponding possible damages in Visp.

Contents

1   Introduction

Seismic risk assessment covers a large number of research fields in geology, seismology, geotechnics, structural engineering, etc. They provide interdependent analysis tools that need a common set of parameters. Therefore, a collaborative work especially between geologists, seismologists and structural engineer is necessary to lead to relevant and coherent methodologies. This is one of the purposes of the COupled seismogenic GEohazards in Alpine Regions (COGEAR) project. This report presents the results for module 1c entitled "Vulnerability and risk" led by IMAC laboratory at EPFL Lausanne. The goal of this module is to define the building stock of the target city of Visp (Valais) (Task 1c.1) and propose vulnerability functions (or fragility curves) to characterize the probability of each building class to be damaged for a given ground motion (Task 1c.2). Therefore, using these vulnerability functions, the hazard results (Modules 2 and 3) and the tools developed in Module 1, a complete methodology of seismic risk assessment will be proposed (Task 1d).

Seismic vulnerability assessment in a given area requires previously the knowledge of the distribution of the building stock. Several attempts to assess and classify the Swiss building stock have been already been made [Brennet et al., 2001, Belmouden and Lestuzzi, 2005, Michel et al., 2008]. In any case, on-site surveys have to be conducted in the study-area to collect data about the constructions. The Visp City is an industrial town located in the Rhone Valley. It is typical of the Swiss cities in terms of number of inhabitants (about 8000), distribution of the building stock and regarding its position in an alpine valley. This city is located in the 3b zone of SIA261 design code with a ground acceleration of $1.6\,\mathrm{m/s}^2$, i.e. in the highest Swiss seismic zone that can be considered as moderate. Moreover, a microzonation exists showing large amplifications on the Rhone sediments [CREALP, 2005] compared to the ground motion on the rock (old city-centre). The major Visp earthquake of 1855 [Fritsche et al., 2006] (Intensity VIII in Visp) hit severely the city, even if the Rhone valley was not settled at that time.

In this report, the first part (section 2) describes the building stock found in Visp and large-scale empirical methods are applied to estimate damages for a given scenario and compare with the 1855 Visp earthquake. Then, the study focuses on typical buildings studied in the two last years, including 5 buildings in Visp. The buildings are described (section 3) and the results of in situ dynamic tests for Visp buildings are summarized (section 4). Reference is made to Michel et al. [2008, 2009a] for detailed analysis of other buildings. A modelling strategy coupled to a probabilistic framework is proposed, in order to compute fragility curves of two particular types: stone masonry structures with rigid floors (M3-2i) and modern masonry structures built before 1970 (M6c1) (section 5.2).

2   Building inventory (Task 1c.1)

2.1   Analysis method and data storage

In order to determine the characteristics of Visp building stock, 381 buildings were surveyed. Data on their geometry, material quality and environment were collected by IMAC in approximately 5 days. These data are related to their seismic vulnerability (material quality, stiffness, etc.), to non-structural elements (chimneys, balconies... that could fall on people in case of earthquake) and to their architecture in order to relate them to a particular building class. Indeed, Michel et al. [2008] developed a classification of the Swiss building stock with the assumption that buildings of the same classes have a similar behaviour to strong ground motions. In that case, detailed analysis of each class and the distribution of the classes among the city allows to fully estimate the seismic risk. The building class according to this typology as well as to the EMS classification [Grünthal et al., 1998] has been deduced for each surveyed structure.

In order to be retrieved on the COGEAR website, the data are stored in a PostgreSQL database hosted by a server in the IMAC laboratory that distributes PostGIS (Geographic Information System) layers. These layers can be remotely visualized on a GIS software as well as on the COGEAR portal together with data on seismicity, slope instabilities etc. A layer called 'survey' contains all the surveyed data (section 2.2). Additionally, estimations of the seismic vulnerability using empirical methods are directly computed in the database and the results provided the same way (see section 2.3).

2.2   Distribution of the building stock

Visp used to be a small burg located in a strategic point at the confluence of Saas and Rhone rivers. Until the end of the XIXth century, many houses were made of wood whereas the houses of Burgers were made of stone masonry with wooden floors. In 1855, Visp suffered the greatest earthquake of the last 300 years in Switzerland, with a magnitude estimated to 6.4 and an Intensity in Visp of VIII on the EMS-98 scale [Fritsche et al., 2006]. In 1909, the Lonza chemical industry set up in Visp so that the population and therefore the building stock grew in the direction of the Rhone valley. However, the new buildings are still made of stone masonry. After 1945, the growth accelerate and the whole Rhone Valley is settled at the end of the 1970s. The new buildings are made of RC walls or brick masonry walls with stiff slabs. Nowadays, Visp still has its old city-centre on the rock site and the buildings of the XXth century spread over the Rhone valley (Fig. 1). The chemical industry buildings of the Lonza company are also located on the Rhone sediments, but are not studied in this report.

Fig. 2 shows the evolution of the city from the centre to the suburbs. In Visp, the old town appears clearly on the rock site, whereas the suburbs expanded to the Rhone valley. Most of the buildings of the city (60%) were constructed after 1945.

The distribution of number of storeys (Fig. 3) is also coherent with history. Most of the buildings have around 2-3 storeys, 4-5 storey-buildings are also common, and there are only few high-rise buildings. It may be a general tendency in Switzerland.

The distribution of the main building types is presented in Fig. 4. There are not enough studied buildings to account for a more refined typology. Masonry buildings account for approxi-
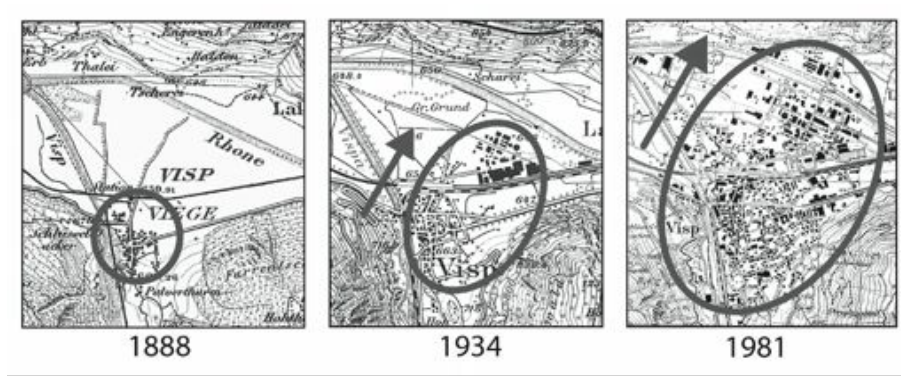
Figure 1: Development of the city of Visp from 1888 (after the 1855 earthquake) to 1981.

mately 2/3 (63%) of the buildings. A large part of stone masonry structures (approximately 1/2) are historical buildings of the old city-centre. The other great part of buildings are RC structures, especially made of shear walls (28%). Excluding some industrial steel structures, we can also remark the presence of 5% of wooden buildings, related to the construction tradition of the mountainous surroundings.

The observation of many buildings allow us to better select typical buildings that can be studied in a more detailed way (see section 3).
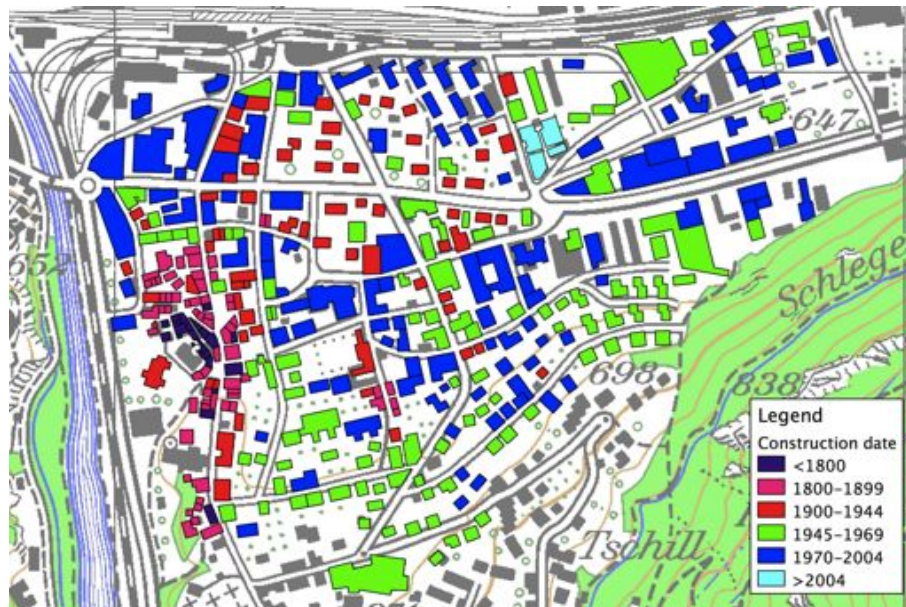
(a)

Visp
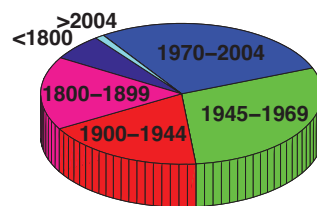
(b)

Figure 2: Distribution of the construction years of buildings in Visp from the survey data.

(a)

(b)

Figure 3: Distribution of the number of storeys of buildings in Visp from the survey data.

(a)

(b)

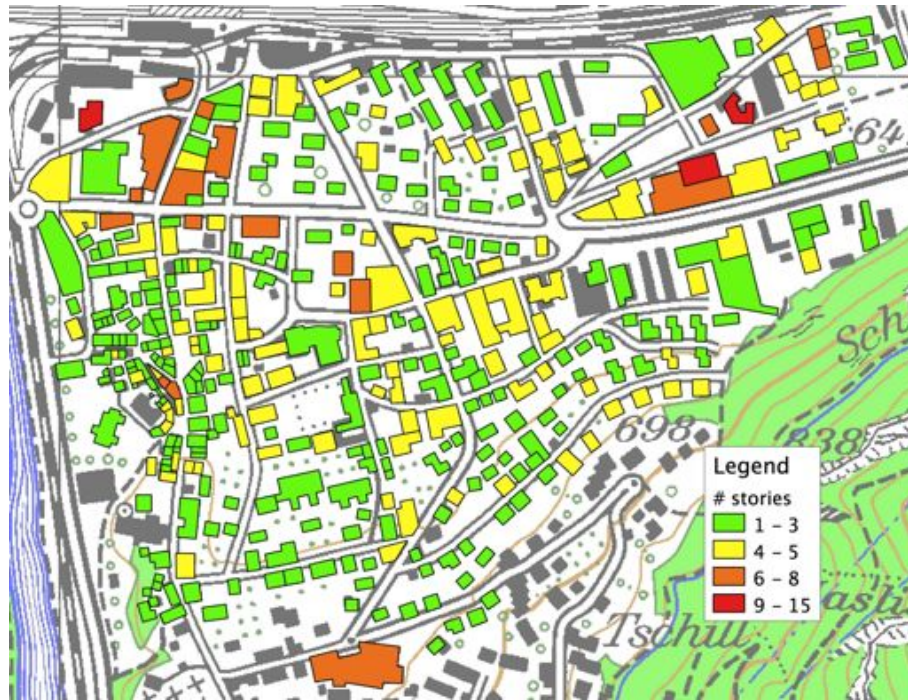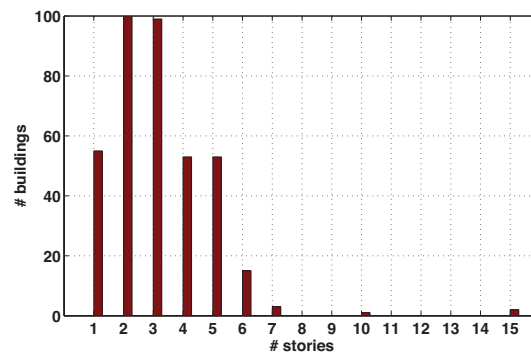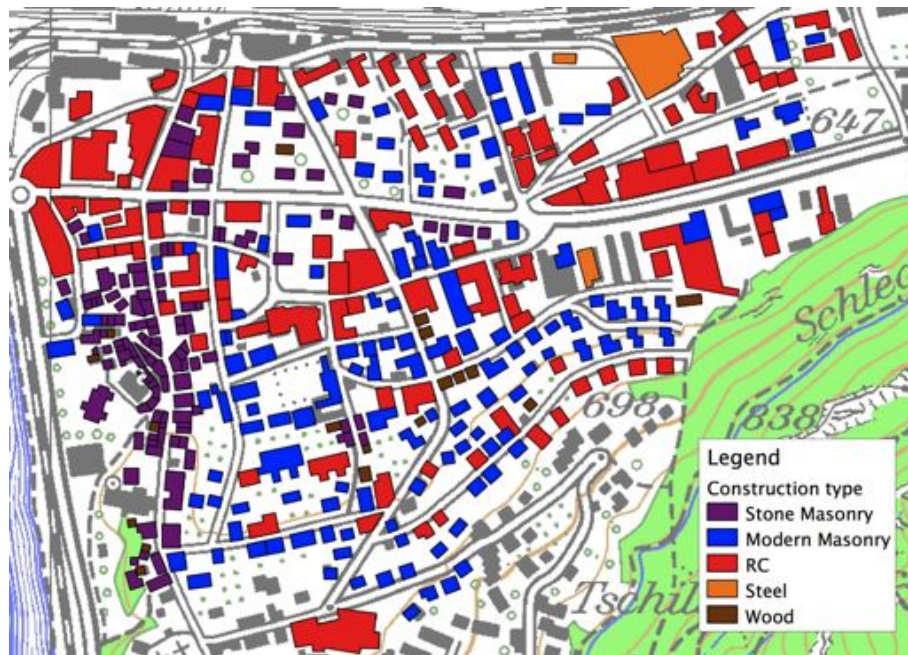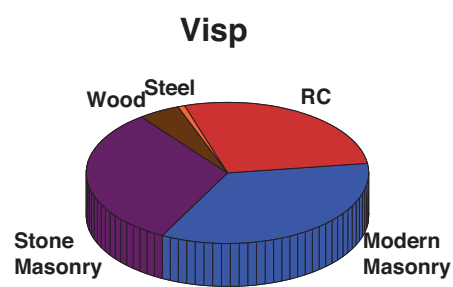Figure 4: Distribution of the building material in Visp from the survey data.

2.3   Empirical Vulnerability and Risk

Surveys at the city-scale also lead to a first estimation of the seismic vulnerability of the city by applying so-called empirical methods. These methods were first proposed in the US after the 1971 San Fernando earthquake [Calvi et al., 2006]. They use statistical data of observed damages to propose vulnerability models based on simple characteristics as the construction material, the geometry, the environment, etc. Two methods were selected according to the numerous methods available in the literature and applied to the survey data: the VulneRAlp method [Guéguen et al., 2007] based on the Italian methods but simplified for the case of Grenoble and the Risk-UE LM1 method [Milutinovic and Trendafiloski, 2003] developed in the frame of a European project by Italian researchers [Lagomarsino and Giovinazzi, 2006]. They are both based on a vulnerability index (VI) that ranges from 0 (not vulnerable) to 100 (very vulnerable) or 0 to 1. Fig. 5 shows the vulnerability index for the city of Visp. These values are only valid on average, not for a particular building. Therefore, zones based on the parameters surveyed in section 2.2 were delimitated. At a first glance, it is clear that Risk-UE and VulneRAlp VI are not comparable, even if they are scaled the same way. Indeed, this parameter gives only a relative value of the vulnerability of each structure. The important parameter is the damage for different Intensity values of earthquake scenario. The results show that city-centre is the most vulnerable.

(a)   (b)
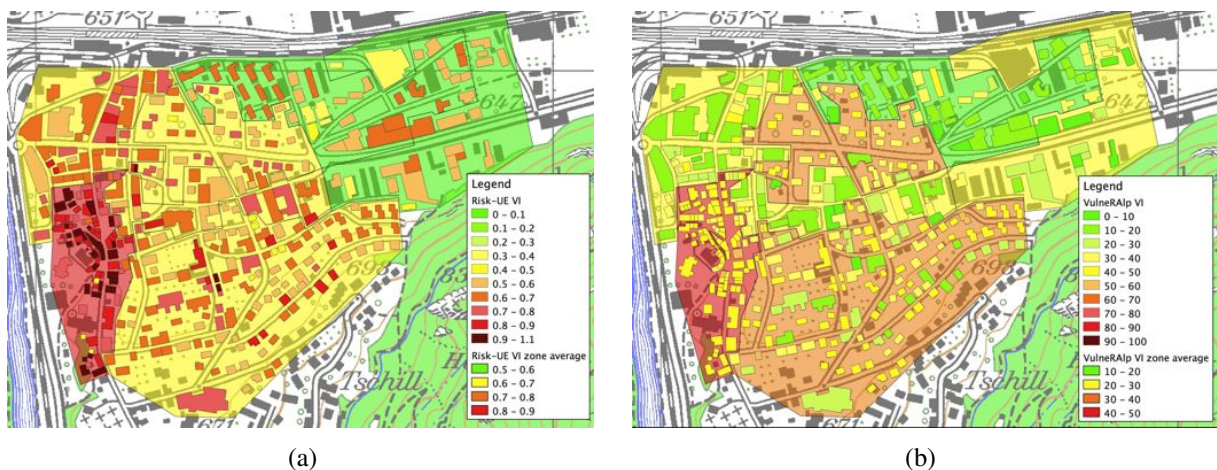
Figure 5: Vulnerability Index (VI) of the city of Visp according to the (a) Risk-UE LM1 and (b) VulneRAlp methods.

In the empirical methods, a relationship is given between the vulnerability index and the damage grades for an earthquake of a given intensity (EMS-98 scale). The results for an Intensity $VIII$ earthquake are displayed on Fig. 6. The average damage grade in the city-centre of Visp is 3 in both methods. However, for the other zones Risk-UE method predicts lower damages than VulneRAlp method. This intensity corresponds to the 1855 earthquake for which historical data are available. Using these data, Fritsche et al. [2006] give an average damage grade of 3 for the city that was there at that time. However, they showed that many structures were in damage grade 4 and several structures fully collapsed that is not predicted by the empirical methods (Fig. 7).

Another sorting method is proposed by the Federal Office for the Environment called OFEV

Figure 6: Damage Grades in case of Intensity $VIII$ earthquake of the city of Visp according to the (a) Risk-UE LM1 and (b) VulneRAlp methods.
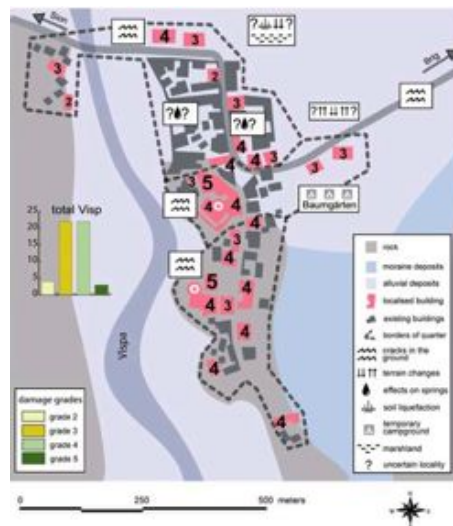

Figure 7: Damage of the 1855 Visp earthquake reconstructed using historical documents. From Fritsche et al. [2006]

step 1 method [Kölz and Duvernay, 2005]. This method, based on risk, aims at sorting buildings to decide the most critical to study in deep. In this study, the collapse probability (WZ) is displayed (Fig. 8). On the contrary to VulneRAlp and Risk-UE, its value is not scaled. The results of this method show a quite different image of vulnerability of the city. Additionally to the old city-centre, many buildings in the train-station zone i.e. on bad soil-conditions, are also to be considered in priority.

Figure 8: Collapse probability (WZ) of the city of Visp according to the OFEV sorting method.

The vulnerability and risk analysis at large-scale using empirical methods give a first insight of the distribution of the vulnerability in a city. However, the results for a given building cannot be used and more detailed analyses are needed. The comparison with the 1855 earthquake displays different damages than what is predicted by methods based on Italian data. This also shows that the particularity of Swiss building stock do not allow the direct use of results from other countries with different building classes [Michel et al., 2008]. Moreover, hazard is estimated using physical parameters such as spectral acceleration or displacement that cannot be used in such empirical methods. The available microzonation shows large amplifications in the Rhone Valley that are therefore not accounted for in these computations. Hence, structures in this zone are likely to be more damaged than expected in the displayed maps. These results show that more adapted methods, based on the real behaviour of existing buildings are needed to really estimate the vulnerability and risk. Therefore, based on case studies, new vulnerability assessment methods are developed in this report.

3 Typical buildings

During the last two years of the COGEAR project, data on many buildings were collected to improve the knowledge on seismic vulnerability of existing buildings in Switzerland. All the buildings studied during that period of time are summarized in Tab. 1. This report focuses on several building classes and does not develop studies for all the structures. References for detailed studies are also given in this table.

Two building classes were particularly studied: stone masonry buildings of the 1920s-30s with RC floors (M3-2i type following Michel et al. [2008]) and clay brick masonry buildings of the 1950s-60s with RC floors (M6c1 type following Michel et al. [2008]). The study of respectively 4 and 3 structures using in situ dynamic tests, numerical and analytical modelling (see section 4 and 5.1) allowed to derive fragility curves for each class (section 5.2). Moreover, mixed structures of brick masonry and RC walls (RCM type) and individual modern brick masonry houses (M6ind type) are also presented in this section and in situ dynamic tests of these structures are developed in section 4. The main issues regarding seismic vulnerability of these classes are exposed. The majority of these structures is located in Switzerland, except two structures studied during the second SGEB survey after the April 2009 L'Aquila earthquake [Michel and Oropeza, 2009]. Five structures, described in more details, are located in Visp.

#	Type	Location	Name	# st.	Cstr. date	Reference
1	M1	Sion (VS)	N.-D. Valère		XIth	Michel [2009]
2	M1i	Visp (VS)	Courthouse	3	1699	
3	M3-1i	Visp (VS)	City Hall	3	1900	
4	M3-2i	Rocca di Cambio (Italy)	Saas Fee	3	1942	Michel and Oropeza [2009]
5	M3-2i	Sion (VS)	Chateauneuf 1	4	1920s	Michel et al. [2009a]
6	M3-2i	Sion (VS)	Chateauneuf 2	4	1920s	Michel et al. [2009a]
7	M3-2i	Lausanne (VD)	Chablais 30	6	1900	Michel et al. [2009a]
8	M6c1	Yverdon (VD)	Jaquier 14-16	4	1940s	Michel et al. [2008]
9	M6c1	Visp (VS)	Litternaweg 7	3	1964	
10	M6c1	Visp (VS)	Litternaweg 9	3	1959	
11	M6c1	Pully (VD)	Chamblandes 56	3	1960s	Michel et al. [2008]
12	M6c1	Bern (BE)	Burgerheim	15	1960s	Oropeza et al. [2009]
13	M6ind	Monthey (VS)	Crochetan 54	1	1940s	Michel et al. [2008]
14	M6ind	Sion (VS)	Ferme Oasis	2	?	Michel et al. [2009a]
15	M6ind	L'Aquila (Italy)	SS80 79	2	1967	Michel and Oropeza [2009]
16	RCM	Delémont (JU)	Morépont 2	7	1978	Michel et al. [2009a]
17	RCM	Sion (VS)	La Butte	7	1970s	Michel et al. [2008]
18	RCM	Visp (VS)	Napoleonstr. 22-26	5	1980s	
19	RCM	Lausanne (VD)	Grey 16-20	5	1970s	Michel et al. [2009a]
20	RCM	Chêne-Bougeries (GE)	Montagne L	7	1968	Michel et al. [2009a]
21	RCM	Chêne-Bougeries (GE)	Montagne I	7	1968	Michel et al. [2009a]

Table 1: Summary of the study-buildings over the last two years. The last column refers to previous or additional studies of the corresponding structure.

3.1 Stone masonry structures with wooden floors (M1, M3-1)

Masonry structures with wooden floors (Fig. 9) are known to be the most vulnerable building class. These types of buildings are not adequately assessed by the current methods. The wooden

floors do not ensure a diaphragm effect, therefore out-of-plane behaviour has to be particularly considered. In situ tests, performed for these two structures, may improve the vulnerability assessment but adequate methods should be developed in the future.

Building #2 is a bourgeois house built in 1699 for the Burgener family in Visp. It is now the courthouse. In 1855, the great Visp earthquake (25/07/1855, Intensity VIII in Visp) collapsed its little steeple. It has not been rebuilt before the 1985-86 restoration. On the left part, arcades have been filled between the 30s and the 1985 restoration. This simple stone masonry structure is made of a 3-story part with an attic and a 5.5-story tower (little steeple) containing the stairway (irregularity in elevation). The two last tower stories have been built in 1985 made of concrete blocks masonry with good mortar. The masonry quality cannot be seen but the construction date implies bad mortar. Tower floors are shifted of a half story compared to the floors of the main part of the building. The floors are made of masonry vaults along the corridors, the arcades and in the staircase which stiffens the structure and of wood beams in the rooms. After the quake, tie rods have been added on the structure, especially through the arcades. The large roof (wood frames) has 2 slopes and 2 little turned-down sides. The cellar is made of masonry vaults and stands at the ground level at the back of the building because of the ground slope. The foundation is on the rock.

Building #3 is the City Hall building of Visp, a simple stone masonry 4-story building (the 4th story being converted attics) from the end of the XIXth century. The quality of the masonry is very good and the wall ties are emphasized at the corner. The floors are made of wood beams. The ground floor is partially buried in front of the building because of the ground slope. There is a basement that has not been studied. In addition to the 4 façades walls, two longitudinal walls with many openings ensure the load bearings also with disseminated transverse walls. Except the ground slope, the building is therefore regular in elevation and quite regular in plan.

Such as for the building #2, cultural heritage structures may present very complex behaviour. A study of N.D. de Valère church (#1) in Sion (Valais) using ambient vibrations Michel [2009] showed that until moderate damages, this structure may behave as a whole with complex modes. The dynamic behaviour under low vibration may therefore control the seismic demand, at least for the first damage grades. This may therefore be an approach complementary to mechanical methods based on the plastic theory [Devaux, 2008]. This is also an ongoing research topic.

Figure 9: Picture of the stone masonry buildings with wooden floors (#1,2,3).

3.2   Stone masonry structures with rigid floors (M3-2i)

This type is particularly studied in sections 5.1 and 5.2. The rigid floors provide a better deformation capacity since displacement is distributed over the walls and out-of-plane behaviour is avoided. The whole structure is also slightly stiffer thanks to these floors. The stiff floors are often added during retrofitting works like recently for building #7. Four study-buildings belong to that class of buildings (Fig. 10).

Figure 10: Picture of the stone masonry buildings with rigid floors (#4,5,6,7).

3.3   Modern masonry structures built before 1970 (M6c1)

This type (Fig. 11) is also particularly studied in section 5.1 and 5.2. The three first buildings, with a similar geometry, were already presented in Michel et al. [2008]. They have regularly distributed URM walls, 3 to 4 RC floors ensuring a diaphragm effect. Their basement is generally half-buried. Their slightly sloppy roofs with 4 sides are characteristics of this type. They are widespread in Switzerland and therefore interesting to study in detail.
Particularly buildings #9,10 are similar 3-storey buildings located Litternaweg 7 and 9 in Visp built respectively in 1964 and 1959. They are 8.9 by $23\,\mathrm{m}$ and 8.7 by $22.5\,\mathrm{m}$, respectively (storey height: $2.6\,\mathrm{m}$). The last storey is a converted attic. The façade and inner brick masonry walls are $15\,\mathrm{cm}$ thick. Building #9 has an additional $18\,\mathrm{cm}$ thick transverse firewall but #10 has more longitudinal walls.

Another structure of this type is studied here (#12) but its dimensions make the comparison with the three preceding buildings difficult: the Burgerheim tower, a 15-storey building of in the 1960s in Bern. This structure has been studied in the frame of a Master project [Bigler, 2009] and a journal paper [Oropeza et al., 2009] is in preparation.

Figure 11: Picture of the URM buildings built before 1970 (#8,9,10,11,12).

3.4   Brick masonry houses (M6ind)

Data on 3 brick masonry single-family detached houses with stiff floors are available but are not detailed in this report (Fig. 12). This building type may be interesting to study in more detail in the future since it is widespread in Switzerland. However, the height of such buildings make them relatively safe to earthquakes in Switzerland.

Figure 12: Picture of the single-family URM buildings (#13,14,15).

3.5   Mixed masonry and RC walls structures (RCM)

This class appears to be broadly distributed across Switzerland (Fig. 13). The difficulty in the study of these structures is to determine the position of the masonry and RC walls since plans are seldom available. Their floors are generally cast-in-place RC elements ensuring a diaphragm effect and their basement RC walls box-section for nuclear protection because of civil protection requirements at that time. Their roof are flat. These structures are not studied with the analytical methods in the following. Adapted methods should indeed be developed and need further research efforts. Indeed, it is not straightforward to account for both RC and masonry walls.

One is a 5-storey building (#18) located Napoleonstrasse 22-26 in Visp. It is 15 by $55\,\mathrm{m}$ and divided in 3 modules without joints. The load bearing system is made of both RC walls enclosing the stairwells and façade brick masonry walls. It has no basement.

Figure 13: Picture of the mixed RC and URM walls buildings (#16,17,18,19,20,21).

4 Dynamic tests on structures

In situ dynamic tests were performed in the structures presented in section 3. These tests allow to determine the dynamic behaviour of structures under low vibrations. The resulting frequency values are summarized in Tab. 3. Only tests on buildings of Visp are detailed here.

4.1 Experiment description

Ambient Vibrations

Structures are permanently subjected to ambient vibrations due to:

- ground ambient vibrations in a wide frequency range,

- atmosphere, i.e. wind, at low frequencies,

- internal sources (pedestrians, machines like lifts...), with great amplitudes at well defined frequencies.

Considering the necessity for Operational Modal Analysis, i.e. under ambient vibrations, to have a white noise input, ground ambient vibrations is the only beneficial loading. It results from large-scale oceanic and atmospheric conditions at frequencies below $0.5\,\mathrm{Hz}$, local meteorological conditions (wind and rain) at frequencies around $1\,\mathrm{Hz}$ and human activities (industrial

machines, traffic...) at frequencies above $1\,\mathrm{Hz}$ [Bonnefoy-Claudet et al., 2006]. In addition to this quasi-stationary signal, natural or anthropogenic transients can affect the stationarity of the signal and should not be used in the analysis.

Material

Simultaneous recordings in several points of all the structures was possible thanks to the material of the Swiss Seismological Service (SED) and the Seismic Risk team of LGIT Grenoble. For buildings #2,3,9,10 and 18, the recordings were digitized using Quanterra Q330 stations with Lennartz 3C $5\,\mathrm{s}$ sensors synchronized by GPS. During the post-earthquake survey in L'Aquila, we used only one Quanterra digitizer and a Lennartz $1\,\mathrm{s}$ sensor. The other structures were recorded using a Cityshark 2 station [Chatelain et al., 2000] allowing the simultaneous recording of 6 triaxial sensors. Two sets of sensor were used depending on the study: 6 Lennartz 3D $5\,\mathrm{s}$ seismometers for buildings 5, 6, 7 (2 times) and 16 and 4 Lennartz 3D $1\,\mathrm{s}$ for buildings 7 (1 time), 14 and 19 to 22.

Position of recording points

Tab. 2 summarizes the number of points recorded in each structure and in free field. A total of 212 points in structures and 17 points in free field have been recorded.

Courthouse   Ambient vibrations were recorded in 10 different points of this structure and a point in free field during $30\,\mathrm{min}$. One point at each storey in the staircase were recorded and 2 additional points at the second floor to estimate torsion.

City Hall   Ambient vibrations were recorded in 9 different points of this structure during $18\,\mathrm{min}$, 3 points at each upper floor (2 at the last floor) and one at the ground floor.

Litternaweg 7,9   Ambient vibrations were recorded in 8 different points of each structure during 36 and $25\,\mathrm{min}$, respectively, as well as 1 point in free field next to Litternaweg 7. It corresponds to 1 point at each story and 3 points at the last floor.

Napoleonstrasse 22-26   Ambient vibrations were recorded in 15 different points of this structure (2 datasets with a reference point in the stairway #26 at the 4th story) during 33 and $46\,\mathrm{min}$.

4.2   Processing techniques

Spectra

The easiest way to obtain modal information from ambient vibration recordings is to estimate their spectra. We calculate here the Power Spectral Density (PSD) spectra, using the Welch [1967] method. We first select 50% overlapping time windows of 8192 samples using an anti-triggering Short Time Average Long Time Average (STA/LTA) algorithm in order to use only a

#	Building	Points in the structure	Free field points
1	N.D. Valère	33	1
2	Courthouse	10	1
3	City Hall	9	0
4	Saas Fee	1	0
5	Chateauneuf 1	14	1
6	Chateauneuf 2	1	0
7	Chablais 30	16+29+13	0+1+1
8	Jaquier 14-16	14	2
9	Litternaweg 7	8	1
10	Litternaweg 9	8	1
11	Chamblandes 56	11	0
12	Burgerheim	25	1
13	Crochetan 54	5	0
14	Ferme Oasis	7	0
15	SS80 79	1	1
16	Morépont 2	24	1
17	La Butte	8	2
18	Napoleonstr. 22-26	15	1
19	Grey 16-20	18	0
20	Montagne L	21	1
21	Montagne I	18	1
22	Grey 22	13	0

Table 2: Number of recorded points in the study-structures.

stationary signal. Then, the Fourier Transforms of these Hamming windows are averaged and squared. These $42\,\mathrm{s}$ windows at $200\,\mathrm{Hz}$, correspond to a frequency precision of $200/8192 = 0.025\,\mathrm{Hz}$. The peaks in the spectra can be either due to ambient loading, internal sources or structural modes. Very sharp peaks can be removed from the interpretation since they are due to undamped motion that cannot be structural modes. The proposed evaluation of the uncertainties on the peak position in the spectrum does not include epistemic errors, but only the uncertainties due to the windowing process in the spectral estimation.

Frequency Domain Decomposition

In order to extract the modal parameters of the structure (resonance frequencies, damping ratios and modal shapes) from ambient vibration recordings, the Frequency Domain Decomposition (FDD) method [Brincker et al., 2001b] was used in this study. This rather simple modal analysis method allows a real system analysis, i.e. a decomposition of complex modes including torsion, even if they are very close as generally the case in buildings. The three basic assumptions of this method are a white noise input, a low damping and orthogonal close modes. The first assumption can cause some troubles in case of bad foundation soil, whereas the method is generally robust enough. The two last assumptions are generally well verified in buildings. The first step of this method is to calculate the PSD matrices for each dataset. For this purpose, the method explained above is used for each couple of simultaneous recording channels. Given that 18 channels are recorded simultaneously, the size of these matrices is 18x18 for each frequency. The second step is to perform the singular value decomposition of these matrices. Only a limited number of modes (frequencies f_k, mode shape vectors $\{\Phi_k\}$) have energy at one particular

frequency f, so that the greatest part of the singular values are close to 0. The first singular values, averaged over the recorded datasets, are displayed Fig. 14 for building #22 as an example and called FDD spectrum. Brincker et al. [2001b] showed that the magnitude of the first singular value gives a peak for an f value corresponding to a resonance frequency f_k. Furthermore, if in the vicinity of f, if there are only one or two geometrically orthogonal elements, the first two singular vectors are proportional to the modal shapes. In practice, buildings are often equally stiff in both longitudinal and transverse directions so that the first modes in each direction are very close together, including often torsion coupling. Moreover, this method can be enhanced [Brincker et al., 2001a] to select the complete mode "bell", including frequency and damping ratio, by comparing the mode shape at the peak to the singular vectors at the surrounding frequency values. The Modal Assurance Criterion (MAC) [Allemang and Brown, 1982], i.e. their correlation coefficient, is used for this purpose. A point with MAC value with the peak greater than 80% is considered as still belonging to the mode "bell", even if this point is located on the second singular value. The bell is then the Transfer Function of the single degree of freedom (SDOF) system representing the study-mode so that an inverse Fourier Transform leads to the Impulse Response Function (IRF) of the mode. The logarithmic decrement of the IRF gives the damping ratio and a linear regression of the zero-crossing times gives the enhanced frequency. A decision as to whether or not a peak is a structural mode can be taken by considering the extent of the mode "bell", the damping ratio and the shape.

Additionally, we made geometrical computation on the structural modal shapes in order to quantify the effects of torsion and soil-structure interaction. Each shape has been modelled as a 1D (rigid floors) 3 degrees-of-freedom system (X and Y drift and rotation). For that purpose, the centre of rotation is needed. We assumed here that it was located at the centre of the building but a sensitivity analysis on its position can give the uncertainties on the results. The ratios of the 3 DOF at the last floors for the building point with the greatest eccentricity are calculated to estimate the proportion of torsion in the mode (coupled mode).
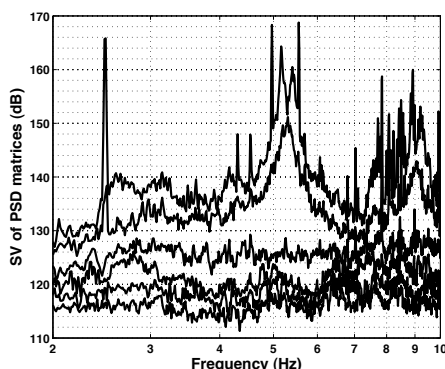

Figure 14: Average FDD spectrum of the recordings in building #2 (Courthouse).

Soil

In addition to reference information about the ground vibrations for Transfer Function estimation for example, ground ambient vibration may also deliver information on soil properties. The

Horizontal to Vertical Spectral Ratios (HVSR), or Nakamura technique [Bard, 2008] is able at some extent to detect the resonance frequencies of soil layers that may produce site amplification in case of earthquake. The square root of the PSD spectra have been smoothed using the Konno and Ohmachi [1998] technique with a coefficient b equal to 40.

4.3 Interpreted Results

Only buildings located in Visp are interpreted here. For the other results, see Michel et al. [2009a].

Courthouse (#2)

The FDD spectra (Fig. 14)) are quite clear and show well the resonances of the structures. However, a lot of undamped peaks, especially at 2.49 Hz but also at 4.31, 4.54, 4.97, 5.55, 7.03, 7.84, 8.08 Hz coming from the human activities can disturb the peaks interpretation. The first structural mode of the Courthouse is the longitudinal bending mode at 5.16 ± 0.02 Hz (Fig. 15). It can be considered as pure bending even if slight transverse and rotation have been calculated. The modal shape shows that the upper part of the tower is much more flexible than the lower part of the building because of the great amplitudes of the last floors. The estimated damping ratio is incredibly low (0.8%). It could be the result of the tower sharpness. The relative displacement of the foundation is found to be less than 1% of the top motion, i.e. negligible as supposed before. The second structural mode, very close from the first, is the first transverse bending mode at 5.41 ± 0.02 Hz. It is pure bending and has the same characteristics as the previous mode. The damping ratio may be a bit larger at 1.3%. The soil-structure interaction is, as well, close to 0. The second bending modes can be found at 8.9 ± 0.1 and 9.2 ± 0.1 Hz. Their decomposition is not parallel to the main directions of the building. The first is more transverse (2/3 transverse, 1/3 longitudinal) and the second more longitudinal (2/3 longitudinal, 1/3 transverse). The relative displacement of the foundation is still found to be negligible.

The frequency ratios between the second and the first resonance frequencies are between 1.6 and 1.8 whereas simple beam models give results between 3 (pure shear) and 6.3 (pure bending) so that these simple models that apply well to reinforced concrete (RC) structures are not valid for masonry buildings with wooden floors. A more exotic mode can be found at 18 ± 1 Hz, the first vertical mode of the building, i.e. a "breathing" mode of the masonry walls.

Without any seismic computation, it is easy, looking at the modal shapes, to understand with the little steeple of the Courthouse collapsed during the Visp earthquake. This elevation irregularity implies very large drifts at the tower top and this part can be ruined quickly. The building has however quite high resonance frequencies (around 5 Hz) and is therefore relatively stiff. The very low damping found is probably linked to the sharpness of the tower, whereas the damping of the main part of the building could be higher. It should however be taken into account in the seismic analysis.

City Hall (#3)

The first structural mode of the City Hall is the first transverse bending mode at $6.48 \pm 0.03\,\mathrm{Hz}$ with a damping ratio of $1.5 \pm 0.4\%$. It can be considered as a pure bending mode (Fig. 15) even if a slight torsion component exists. The modal shape looks like a simple bending beam as found generally for the masonry wall buildings. The second structural mode is the first longitudinal bending mode at $7.7 \pm 0.2\,\mathrm{Hz}$. It is a coupled mode (2/3 bending, 1/3 torsion). The damping estimation is approximately the same as the previous mode but undamped peaks disturb the computation. This is a very stiff and regular structure. The transverse direction, as suggested by the geometry, is the most flexible direction and therefore the most vulnerable to earthquakes. We found a torsion component in the longitudinal direction, which means an eccentricity of the centre of rigidity in the transverse direction but it should not be important for the seismic assessment because of the high frequency of the longitudinal mode.

Litternaweg 7 (#9) and 9 (#10)

The spectrum of building #9 does not show clear peaks because of the low signal-to-noise ratio. Transfer functions have been calculated to estimate the resonance frequencies. The first transverse mode (Fig. 15) at $4.6 \pm 0.4\,\mathrm{Hz}$ is slightly coupled with torsion. The relative displacement of the foundation is estimated at $15 \pm 5\%$ of the top motion. The first longitudinal mode at approximately the same frequency $4.6 \pm 0.3\,\mathrm{Hz}$ is also coupled with torsion (15-30%). The relative displacement of the foundation is of the same order of magnitude (10%). The modal shape of the transverse mode is more in shear indicating that the horizontal stiffness dominates the vertical stiffness, whereas the longitudinal mode is more in bending, indicating the predominance of the vertical stiffness. The low quality of the spectrum did not allow estimating damping ratios.

The building #10 shows the same features as building 6 except that its first modes are not so close at 4.4 ± 0.1 and $5.1 \pm 0.1\,\mathrm{Hz}$, respectively in the transverse and longitudinal directions. Moreover, these modes are pure bending and not coupled with torsion.

Napoleonstrasse 22-26 (#18)

As for buildings #9 and 10, only transfer function estimations could give the resonance frequencies of building #18. The transverse bending mode at $4.7 \pm 0.1\,\mathrm{Hz}$ is slightly coupled with torsion (Fig. 15). The longitudinal mode at $5.96 \pm 0.05\,\mathrm{Hz}$ is strongly coupled with torsion. The relative displacement of the foundation at this frequency is large, about 30%, but not reliable.

4.4   Discussion

The study-buildings are of very different building classes but general conclusions can be made. Concerning the frequency values, Michel [2007] estimated a frequency-height relationship for RC wall buildings in Grenoble and Nice (France). The resulting equation is $T = 0.013 * H \pm 0.08$. The first longitudinal and transverse frequencies of the study-buildings are displayed in Fig. 16 regarding this equation. All the structures may belong to the distribution found for RC wall structures. The greatest difference comes from the first mode of the Burgerheim tower
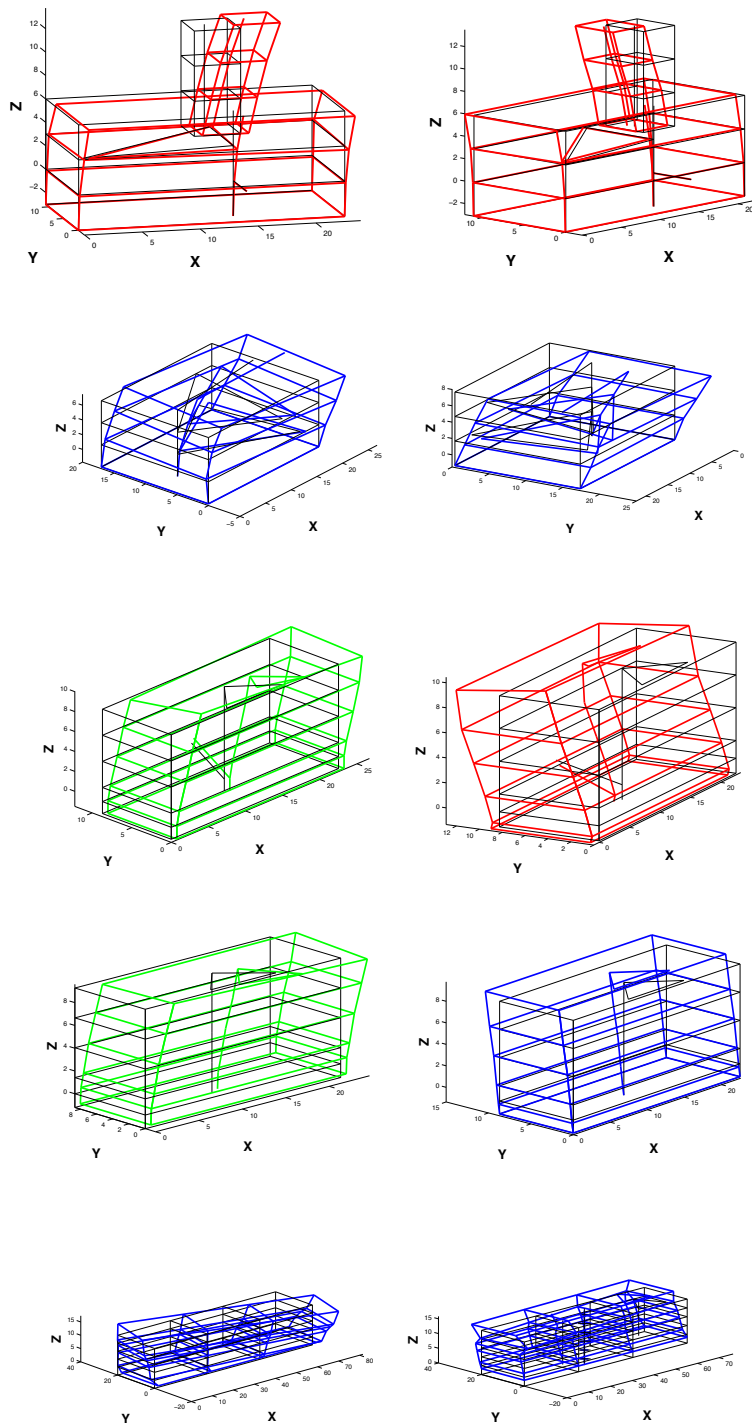
Figure 15: Estimated modal shapes of the first longitudinal and transverse modes of Visp buildings #2, 3, 9, 10 and 18.

#	Building	# st.	1st **Trans.**	1st **Long.**	1st **Tors.**	Coupling
1	N.D. Valère		2.58	4.08		No
2	Courthouse	3	5.41	5.16		No
3	City Hall	3	6.48	7.7		No
4	Saas Fee	3	8	6.9	11	Slight (Long.)
5	Chateauneuf 1	4	4.78	6.73	8.5	Strong (Long.)
6	Chateauneuf 2	4	3.5	5.5		Strong (Long.)
7	Chablais 30 (final)	6	3.26	3.41	4.74	Slight (Both)
8	Jaquier 14-16	4	5	5		Unknown
9	Litternaweg 7	3	4.6	4.6		Slight (Both)
10	Litternaweg 9	3	4.4	5.1		No
11	Chamblandes 56	3	6.47	5.77	7.6	Strong (Both)
12	Burgerheim	15	1.22	1.73	2.21	Strong (Both)
13	Crochetan 54	1	10.0	12.5	17	Slight (Both)
14	Ferme Oasis	2	5.8	5.5		No
15	SS80 79	2	10.5	8.55	12.6	No
16	Morépont 2	7	4.24	4.09	4.90	Slight (Trans.)
17	La Butte	7	3.52	3.7	3.81	Slight (Trans.)
18	Napoleonstr. 22-26	5	4.7	5.96		Strong (Long.)
19	Grey 16-20	5	6.38	4.51		No
20	Montagne L	7	3.72	3.29		No
21	Montagne I	7	2.93	3.15		Slight (Long.)

Table 3: Fundamental frequencies (Hz) of the study-buildings.

(#12). It is strongly coupled with torsion and lead to a much greater period than other structures of the same height. This may also be due to masonry walls that are more flexible than RC walls. On average, masonry structures are mostly in the upper part of the distribution, i.e. more flexible than the relationship valid for RC structures.

The study of stone-masonry structures with RC floors shows that rigid floors eliminate internal deformations of the slab but may let torsion develop if eccentricities exist. Moreover, the RC floors rigidify noticeably the whole structure (approximately 40% in stiffness for building #7).

The shape in height of masonry structures cannot be easily compared to standard beams (cantilever or shear). Walls provide generally a large vertical stiffness leading to a cantilever beam behaviour but RC floors make the horizontal stiffness comparable to vertical stiffness. For RC structures there is even a wider range of possibilities. Very weak directions such as the longitudinal direction of long buildings may even show a shear behaviour.
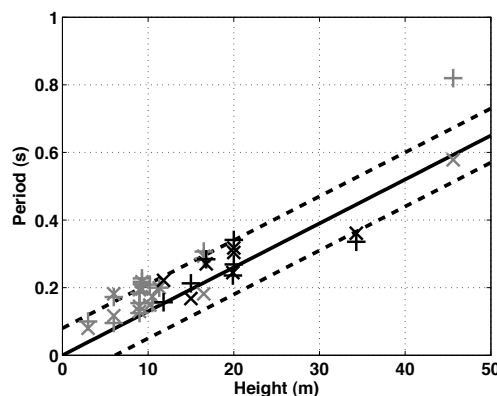
Figure 16: Periods of the study-buildings as a function of building height compared to the relationship found on RC wall structures with its standard deviation. Grey and black stand for masonry and RC structures, respectively. Plus and cross symbols stand for transverse and longitudinal directions, respectively.

4.5 Opportunities of permanent instrumentation

Currently, no building is instrumented in Switzerland on the contrary, for example to California (hundreds of instrumented buildings by the CSMIP) or France (3 instrumented buildings by the national strong motion network `http://www-rap.obs.ujf-grenoble.fr`). The building instrumentation can follow different objectives:

- structural health monitoring, i.e. following the dynamic properties of structures due to natural variation and damage

- earthquake recordings for a better understanding of the structural behaviour under earthquake

Currently, no masonry structure is instrumented across the world, whereas they are the most important in Switzerland. It would be necessary to record earthquakes in such structure to better

constrain the model used in seismic analysis. Therefore, it is proposed to instrument a masonry structure on bad soil condition such as building #9 or 10. Moreover, Fig. 17 shows that the noise level at the top of the structure is enough to be recorded by an Episensor acceleromtric sensor [Clinton, 2004]. To produce this figure, the recordings have been processed following McNamara and Buland [2004] implemented in Matlab (equivalent of PQLX software). Therefore, the permanent recordings could also be used as structural health monitoring, despite the limited height of the building.

Following this recommendation, a temporary accelerometric station was installed in the neighborhood of these structures by the Swiss Seismological Service in the frame of the CO-GEAR project, before additional fundings can be found to instrument the structure.
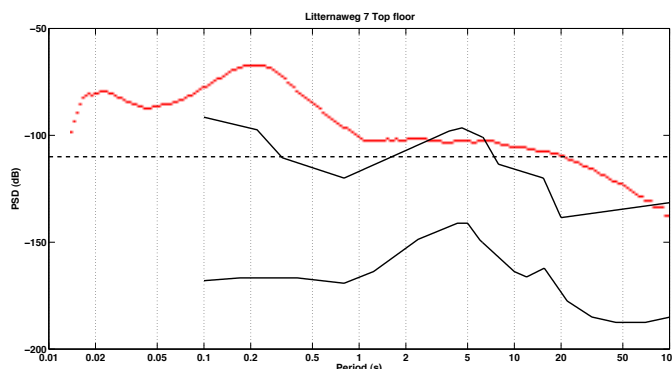
Figure 17: Spectrum of a top floor noise recording in transverse direction in building #9 (Litternaweg 7) in red and comparison with Episensor resolution (dashed black line) and the high and low noise models (solid black lines).

4.6   Implications for earthquake engineering

Ambient vibration measurements give the real dynamic behaviour of structures under low vibrations. This behaviour is depending on structural properties (geometry, material properties...) but is also affected by environmental parameters such as temperature, soil-structure interaction, by the participation of non-structural elements, etc.. Clinton et al. [2006] showed that the vibration frequency of the Millikan Library in California changed of $\pm 4\%$ due to environmental parameters. Moreover, Hans et al. [2005] showed that light non-structural elements such as windows, light partition walls, etc. accounted for 2 to 4% in the resonance frequency of RC structures. They also showed that heavy precast facade elements of masonry infill panel had a great importance in the total frequency of theses structures, up to 20%. In a model, even refined, some of these factors are not taken into account (non-structural elements...) first because it is time-consuming and second because they do not participate to the lateral resistance in case of strong earthquake. When comparing to ambient vibration results, the modeller has to be aware of all the assumptions he made.

Moreover, it has been shown by many authors that the resonance frequency of structures decreases when amplitude increases first in the elastic and then the plastic domain. In the latest, this frequency drop is due to increasing damage. In earthquake engineering assessment, the key-parameter is the elastic frequency, i.e. the frequency before the drop due to damage.

Michel et al. [2009b] showed however that a frequency drop due to non-linearity mainly in the structural elements (and not the non-structural elements) occurs and depends mainly on vibration amplitude. For unreinforced masonry structures, Michel et al. [2009b] estimated a 1/3 frequency drop up to the elastic limit. This may not be the same for stone masonry or RC structures but it gives an idea of the difference between ambient vibration results and models used for earthquake engineering purposes. In any case, the resonance frequency in models must always be smaller than the one found under ambient vibrations. It is however hardly smaller than the half of it. It should again be reminded that for force-based approaches, a conservative estimation is a higher frequency (lower period), whereas for a displacement-based approach, a smaller frequency (higher period) should be preferred.

Modal shapes do not suffer major variations in the elastic domain. Even damage detection is very hard using this very robust parameter. Therefore they can really be compared to models, taking the assumptions on the model into account. The only problem is that, under ambient vibrations, all the fastened elements participate to the stiffness (precast elements, infill panels, thin joints may not work...) whereas under earthquake their connection may break easily.

There are however no evidence that damping ratio found in ambient vibration experiments can be used for earthquake engineering. Research is going on in this topic.

In conclusion, the real behaviour of structures under earthquake is not very different from ambient vibration behaviour and they can be used to validate model when taking all the above parameters into account. The comparison between ambient vibrations and earthquake engineering models can been done using the 1/3 reduction. It should however be noticed that the comparison led to significant differences for building #16 that could not been explained yet. This would be due to a better quality of brick or the presence of more RC walls than expected.
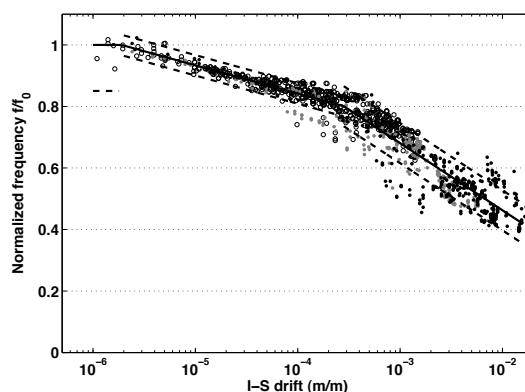

Figure 18: Frequency drop relationship found for clay masonry with the 80% confidence interval.

5   Derivation of fragility curves (Task 1c.2)

5.1   Modelling

Section 2 showed that empirical methods were not enough to study the vulnerability of existing buildings and that we should account for the physics of structural dynamics. Experimental data collected in section 4 showed what were the important features of dynamic behaviour of existing buildings. In order to assess the structural vulnerability, models to estimate earthquake response and performance of structures are needed. Moreover, inelastic studies for vulnerability assessments should be computed a large amount of times and therefore remain simple. Analytical formulations should therefore be preferred. In this section, buildings of the M3-2i, i.e. stone masonry structures with rigid floors and M6c1, i.e. modern masonry structures built before 1970 (low-rise) classes are studied.

The proposed modelling is based on the work by Lang [2002] adapted to URM structures. This is a non-linear static procedure accounting for an elastic perfectly plastic model of each wall of the structure. The capacity curve is considered to be the sum of the capacity of each wall. The proposed method provides improvements in some of the most important parameters of seismic assessment: the elastic displacement and the fundamental period. Different strength estimations and ultimate drift prediction formulations are also considered. These parameters have a significant influence on the capacity curve.

The elementary capacity curve (each wall) presents a simplified bi-linear behaviour and it is determined by three parameters: the strength of the wall (V_{Rd}), the elastic displacement at yield (Δ_y) and the ultimate drift (δ_u). These curves are computed with respect to the displacements at the top of the building and the corresponding forces. During the plastic behaviour, it is assumed that these deformations occur at the first story.

Lang [2002] proposes to estimate the strength of a wall following the stress-field theory depending on the design strength of the masonry orthogonal and parallel to the mortar bed, the wall length, the thickness of the wall, the normal force and the height of zero moment (h_0). Despite the theoretical basis of the precedent formulation, a scatter in the prediction of strength of masonry walls remains [Fehling et al., 2007, Magenes et al., 2008], thus the Eurocode 6 [European Committee for Standardisation, 1995] formulation is also considered. An additional parameter is introduced: the shear strength under zero compressive stress f_{vk0}.

An improved approach for computing Δ_y and based on the principle of virtual work was used [Oropeza et al., 2009]. Δ_y is generated by the lateral displacement of the walls under a shear load and the impact of rotation of these walls at each storey. It is expressed as a function of the total height of the wall, the height of the pier, the factor form for wall with a rectangular cross section and the effective bending and shear stiffness.

Lang [2002] uses a linear interpolation of few tests results for estimating ultimate drift as a function of the normal stress σ_n, and geometrical parameters such as the height of piers and the length of walls. However, when the experimental database of URM walls is extended, one finds a significant scatter. Therefore, another simple formulation [Michel et al., 2009a] based in a more extensive study of experimental test is proposed. In addition to consider the same parameters used before, it accounts for the strength of masonry f_{xd} and the boundary conditions h_0.

An improved methodology for estimating the fundamental period was used and the results successfully compared to the ambient vibrations. Oropeza et al. [2009] provide a coherent approach for computing T from a modified elastic displacement Δ_y using the Rayleigh quotient. Indeed, it was shown that significant differences for mid- and high-rise buildings can be found when Lang [2002] is used.

5.2   Fragility curves

Currently, vulnerability (or fragility) curves constitute a common representation of vulnerability. These curves represent the probability of exceeding each damage grade considering a given level of loading. As it is done generally in the literature [FEMA, 2003, Milutinovic and Trendafiloski, 2003], the curves are modelled by cumulative log-normal distributions defined by a median and a standard deviation. The median represents (in short) the most probable displacement for which the damage grade is reached and the standard deviation integrates the intrinsic variability of the phenomena as well as the uncertainties in the computations.

Selected parameters

In this study, the loading is represented by the elastic spectral displacement at the frequency of the structure for a 5% damping. Other parameters may be found in the literature such as Intensity, but this parameter is not really relevant for analytical modelling, Peak Ground Acceleration (PGA), etc. The current displacement-based methods (e.g. Milutinovic and Trendafiloski [2003]) use the inelastic spectral displacement, i.e. related to the displacement at the top of the structure, because this parameter is a natural descriptor of the capacity curves. However, its computation while performing a scenario requires the seek for the performance point for the given demand using either the capacity spectrum method [Comartin, 1996] or the EC8 approach [CEN, 2004, Fajfar, 1999]. In these methods, the fragility curves are given together with capacity curves necessary for this computation. The choice in this report is to use the **elastic** spectral displacement by including the EC8 method in the computations of the fragility curves. Therefore, the fragility curves can be straightforwardly used with an elastic response spectrum as an input. Veletsos and Newmark [1960] showed that in average, the inelastic displacement was greater than the displacement of the corresponding elastic system for low periods. This displacement value is therefore converted to the displacement of the equivalent elastic system using Fajfar [1999] relationship (Eq. 1, Fig. 19).

$$R = \frac{\Delta_{elastic}}{\Delta_y} = \left(\frac{\Delta}{\Delta_y} - 1\right)\frac{T}{T_c} + 1 \tag{1}$$

$$\Rightarrow \Delta_{elastic} = \Delta_y\left(\left(\frac{\Delta}{\Delta_y} - 1\right)\frac{T}{T_c} + 1\right) \tag{2}$$

This has an impact only for DG greater than 3 (plastic domain) and for structures with an elastic period lower than T_c taken as $0.5\,\mathrm{s}$ in this study. For greater periods, equal displacement rule applies and therefore the elastic and inelastic displacements can be considered as equal [Fajfar, 1999]. The use of other parameters such as PGA is not natural for such a static displacement-based method.
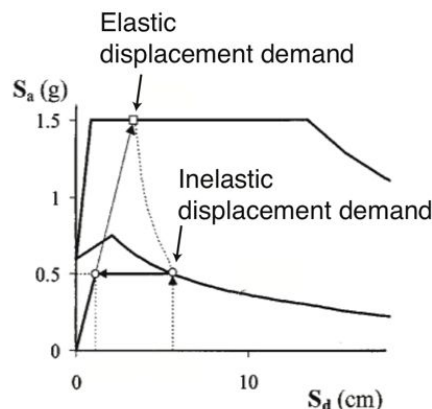
Figure 19: Difference between the inelastic displacement (used as abscissa of the fragility curves in current methods such as FEMA [2003]) and the elastic displacement (used in method 2) following Fajfar [1999] method. From Fajfar [1999].

Qualitative and quantitative damage grades definitions can be significantly different [Hill and Rossetto, 2008]. The damage scale that is used here is the EMS-98 [Grünthal et al., 1998] damage scale having 5 grades: Slight, Moderate, Substantial to heavy, Very heavy, Destruction. The definition of these grades is however based on visual observation in the EMS-98. Their physical definition is based on analytical formulations adapted from Lang [2002]. For this non-linear static procedure, improvements on the estimation of damage grades compared to Lang [2002] is also proposed. On one hand comparisons with Michel et al. [2008] showed that first analytical DG from Lang [2002] are quite conservative. On the other hand, last DG are deeply related to δ_u estimation. The elastic displacement has a significant impact on the damage grade values. In this study, first damage grade definitions were modified.

Since the fragility curves are derived in spectral displacement, one of the main parameter was the height of the structure, which is easy to determine in a large scale study. Therefore, fragility curves of each type are derived for each possible number of storeys, in our case for 3 to 5 storeys, corresponding to mid-rise structures [FEMA, 2003, Milutinovic and Trendafiloski, 2003]. These structures are the most common in Switzerland, especially for the studied classes of buildings. An example of the influence of the number of storeys is presented on Fig. 20. It shows that structures of 3 storeys may already collapse whereas structures of 5 storeys are still not slightly damaged. Frequencies of these structures are also much different.

Models used

The objective of the study of typical buildings is to characterize building classes. The wall distribution of each study-buildings and generic distributions of normal load and height of zero moment are considered. Only the most sensitive direction of each building is used here, whereas the other direction could be representative of other buildings. It is questionable whether the two directions should be used or not, depending on architecture considerations.

In order to derive a probabilistic framework, the variability of certain parameters such as the material properties, and their impact on strength estimations and ultimate drift are studied. Hence, the masonry compressive strength f_{xd} can be defined as a random value following a
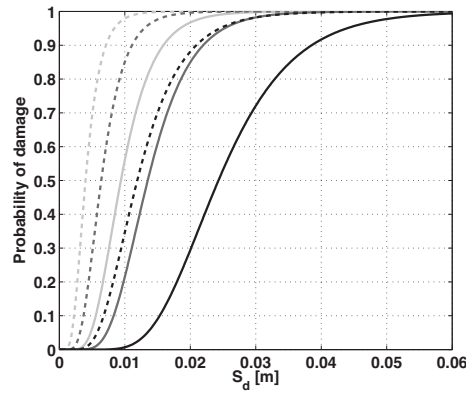
Figure 20: Example of resulting fragility curves for DG 1 (dashed lines) and DG 5 (solid lines) between 3 (light grey) and 5 (black) storeys.

log-normal distribution. Therefore, all the parameters related to this value follow the same random distribution, such as f_{yd}, the elastic modulus E_m, the shear modulus G_m. Similarly, the tensile strength f_t, the shear strength under zero compressive stress f_{vk0}, the effective stiffness $r = \frac{EI_{eff}}{EI} = \frac{GA_{eff}}{GA}$, and the ultimate drift δ_u also follow a log-normal distribution.

Finally, a significant amount of computations need to be performed (about 500) and one obtains log-normal median and standard deviation for the DG. The number of computations depends on the convergence of the obtained results.

Results

M3-2i class   In the stone masonry with stiff floors class (Fig. 21), the weak direction is generally the transverse one since the length of the building is correlated with the length of the walls (box). The frequencies of building #6 and 7 are in good accordance with ambient vibration experiments at yield whereas there are large differences for the two other buildings. The major issue is the material characteristics that are very uncertain. However, ambient vibration value gives still a higher boundary for the frequency value since frequency can only decrease when amplitude increases. Therefore, building #4 is too stiff in the model. The difference of a factor of more than 2 in stiffness between ambient vibrations and modelling for building #5 is also not realistic. The model is therefore too flexible. In conclusion, stone masonry is very difficult to model for earthquake engineers.

The first damage grade occurs for 0.4 to $1.2\,\text{cm}$ depending on the number of storeys. The second damage grade occurs for displacements of 0.4 to $1.4\,\text{cm}$, which seems realistic. For the third damage grade, the method predicts values between 0.6 and $1.8\,\text{cm}$. DG 4 and 5 are generally found between 1.1 and $2.6\,\text{cm}$. It is low for low-rise buildings because of the correction due to the plastic displacement. Indeed, these structures are very high frequency and therefore, a small elastic displacement leads to large inelastic displacements.

The DG values vary significantly with the number of stories. However, the damage grades are very close one another for a given number of storeys indicating a low ductility. This is due to the value of the ultimate drift computed using the various methods and to the fact that

all the plastic displacement is affected to the first storey. This fragile behaviour may be over-conservative.

M6c1 class   For this building class (Fig. 21), the results are in good accordance concerning the resonance frequencies of the structure between the ambient vibrations and the modelling. They are much more reliable because the material properties are better known. The results in terms of fragility curves are however very similar to the previous results.
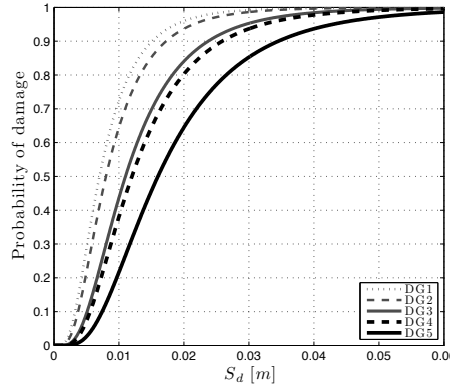

Figure 21: Proposed fragility curves for masonry buildings with stiff floors of 3 to 5 stories.

Comparison with other methods   To be compared with other methods, fragility curves for buildings of 3 to 5 stories mixed, corresponding to mid-rise structures in FEMA [2003], Milutinovic and Trendafiloski [2003], are also derived and shown in Fig. 22. In this figure, the parameter in abscissa is the **inelastic** spectral displacement so that it can be directly compared with FEMA [2003] and Milutinovic and Trendafiloski [2003].

The conclusion here would be that the computations are not very sensitive to the input parameters used but that the results are more depending on the basic assumptions of the method itself. Work is still needed especially to constrain the ultimate drift.

| Class	Storeys	f	μ_1	β_1	μ_2	β_2	μ_3	β_3	μ_4	β_4	μ_5	β_5
M3-2i	3	4.07	0.4	0.53	0.4	0.55	0.6	0.59	0.8	0.50	1.1	0.50
	4	3.03	0.6	0.51	0.7	0.51	1.0	0.53	1.1	0.48	1.5	0.49
	5	1.72	1.2	0.48	1.4	0.45	1.8	0.45	1.9	0.44	2.6	0.45
	3-5	2.96	0.7	0.67	0.8	0.68	1.0	0.69	1.2	0.61	1.6	0.60
M6c1	3	4.28	0.4	0.45	0.5	0.44	0.6	0.47	0.7	0.40	0.9	0.41
	4	3.20	0.6	0.43	0.8	0.39	0.9	0.41	1.0	0.37	1.4	0.38
	5	1.84	1.2	0.44	1.4	0.34	1.8	0.35	1.8	0.34	2.4	0.36
	3-5	3.09	0.7	0.63	0.8	0.58	1.0	0.60	1.1	0.55	1.5	0.55

Table 4: Characteristics of the fragility curves for the building types depending on the storey-number (resonance frequency f in Hz, median μ in cm and standard deviation β) according to the proposed method.
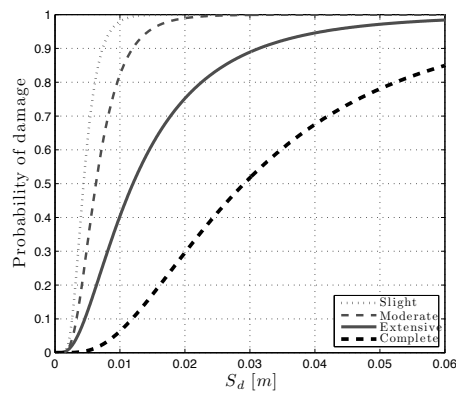
(a) Risk-UE M3.3M class
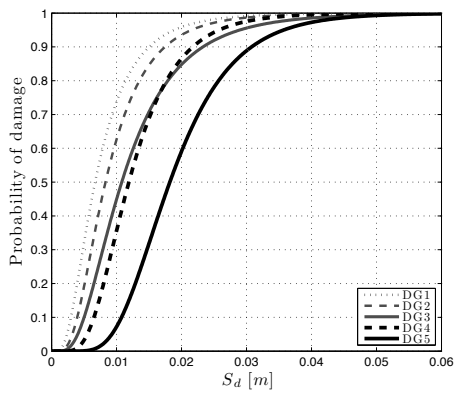
(b) Proposed method M6c1 class 3-5 stories
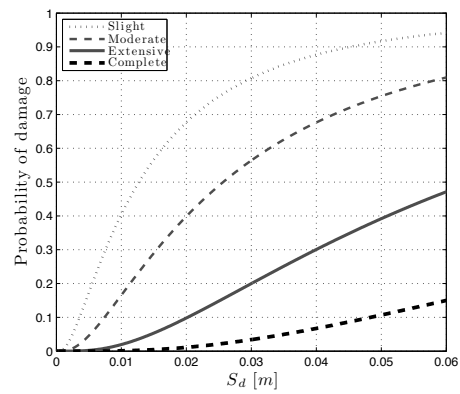
(c) HAZUS URM M class

Figure 22: Fragility curves of URM class with stiff floors from 3 to 5 floors (M6c1) as a function of the **inelastic** spectral displacement and picture of a typical example.

5.3   Discussion for other building classes

The results for two classes showed that neither Risk-UE nor HAZUS provide adapted fragility curves for Swiss masonry structures.

The proposed method can be easily used with the one-family modern masonry houses (M6ind) and mixed RC and masonry structures (RCM). The corresponding fragility curves will be computed in the future.

For masonry structures with wooden floors (classes M1 and M3-1), Risk-UE results seem to be very conservative. The proposed method cannot be directly applied in this case. Especially, the distribution of the height of zero moment will be much different. The walls may behave independently and therefore the distribution of shear forces may be difficult to compute. The frequencies may be obtained using the ambient vibration data.

Concerning the RC structures, they should not be very different from what exist in the US or other European countries. However, a comparison between the European and the US literature shows tremendous differences (Fig. 23). Future studies must decide which curves are best adapted to the Swiss building stock.
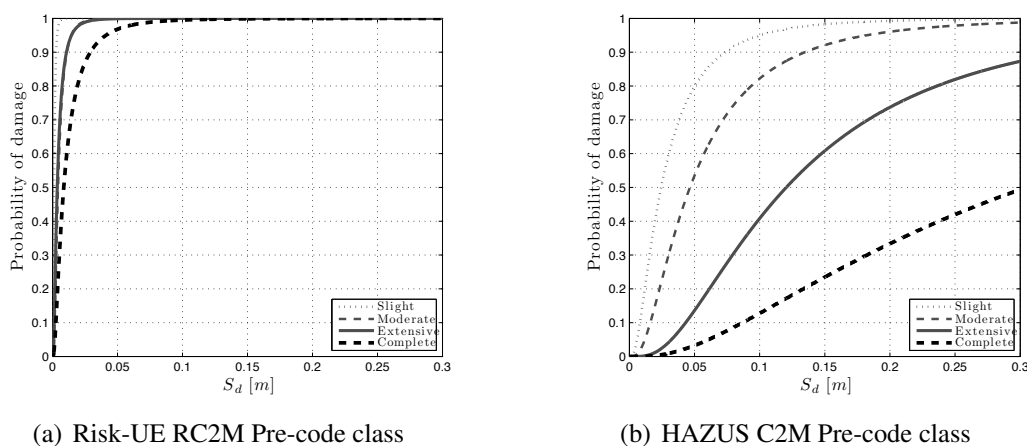

(a) Risk-UE RC2M Pre-code class   (b) HAZUS C2M Pre-code class

Figure 23: Fragility curves of RC shear wall class from 4 to 7 floors from European and US literature.

5.4   Performance of two study-buildings in their environment

It is interesting to estimate the damage that would occur for the study-buildings in case of the elastic displacement demand in the SIA261 code occurs. These results for buildings #9 and 10, for which a microzonation is available [CREALP, 2005] are displayed in Tab. 5.

The microzonation leads to a demand up to approximately $1\,\mathrm{cm}$. The probability of collapse for such a scenario is very high (approximately 50%).

#	Building	Zone	Soil	S_d	P_1	P_2	P_3	P_4	P_5
9/10	Litternaweg 7/9	Micro.	Rhone	0.9	95	90	80	60	40

Table 5: Probability of damage (P in %) for the displacement demand (S_d in cm) in the SIA261 code for Litternaweg structures.

6   Conclusions

This work contributed to increase the level of knowledge on vulnerability of Swiss buildings, especially in the city of Visp. The distribution of the building stock in Visp was investigated and stored in a GIS database. Ambient vibration recordings in different structures were performed for characterizing the dynamic behaviour of these buildings. They are necessary to validate modelling that use very uncertain input parameters for such structures. A new modelling method is proposed and used to compute the fragility curves of masonry buildings with stiff floors. The results are much different compared to HAZUS and Risk-UE and they showed the need for particular assessments, especially for masonry structures.

The proposed fragility curves as well as the building distribution may be used to compute earthquake scenario for Module 1d.

Acknowledgements

References

R.-J. Allemang and D.-L. Brown. A correlation coefficient for modal vector analysis. In *1st International Modal Analysis conference (IMAC)*, Orlando, Florida, 1982.

P.-Y. Bard. The H/V technique: capabilities and limitations based on the results of the SESAME project. *Journal of Earthquake Engineering*, (6):1–2, 2008.

Y. Belmouden and P. Lestuzzi. Elements de typologie du bati existant suisse. Technical Report 5, Office Fédéral des Eaux et de la Géologie, Ecole Polytechnique Fédérale de Lausanne, 2005.

M. Bigler. Vérification de la sécurité parasismique de la tour du Burgerheim à Berne. Master's thesis, Ecole Polytechnique Fédérale de Lausanne, Lausanne, Switzerland, 2009.

S. Bonnefoy-Claudet, F. Cotton, and P.-Y. Bard. The nature of noise wavefield and its applications for site effects studies. A literature review. *Earth Science Review*, 79:205–227, 2006.

G. Brennet, K. Peter, and M. Badoux. Vulnérabilité et risque sismique de la ville d'Aigle. 1ère partie : Inventaire sismique et vulnérabilité du bâti. Technical report, Etablissement Cantonal Vaudois d'Assurance, Ecole Polytechnique Fédérale de Lausanne, 2001.

R. Brincker, C. Ventura, and P. Andersen. Damping estimation by Frequency Domain Decomposition. In *19th International Modal Analysis Conference (IMAC)*, pages 698–703, Kissimmee, Florida, 2001a.

R. Brincker, L. Zhang, and P. Andersen. Modal identification of output only systems using Frequency Domain Decomposition. *Smart Materials and Structures*, 10:441–445, 2001b.

G.M. Calvi, R. Pinho, G. Magenes, J. Bommer, L.F. Restrepo-Velez, and H. Crowley. Development of seismic vulnerability assessment methodologies over the past 30 years. *Indian Society Journal of Earthquake Technology*, 43(3):75–104, September 2006.

CEN. *Eurocode 8: Design of structures for earthquake resistance - Part 1: General rules, seismic actions and rules for buildings*. European Committee for Standardization, en 1998-1:2004 edition, 2004.

J.L. Chatelain, P. Guéguen, B. Guillier, J. Fréchet, F. Bondoux, J. Sarrault, P. Sulpice, and J.M. Neuville. Cityshark: A user-friendly instrument dedicated to ambient noise (microtremor) recording for site and building response studies. *Seismological Research Letters*, 71(6):698–703, 2000.

J. Clinton. *Modern Digital Seismology - Intrumentation and Small Amplitude Studies in the Engineering World*. PhD thesis, California Institute of Technology, 2004.

J. F. Clinton, S. C. Bradford, T. H. Heaton, and J. Favela. The observed wander of the natural frequencies in a structure. *Bulletin of the Seismological Society of America*, 96(1):237–257, 2006.

C. D. Comartin. ATC-40 Seismic evaluation and retrofit of concrete buildings. Technical Report SSC 96-01, Applied Technology Council (ATC), 1996.

CREALP. Soil classes maps of the SIA261 design code, Microzonation Brig-Visp, 2005. URL `www.crealp.ch`.

M. Devaux. *Seismic Vulnerability of Cultural Heritage Buildings in Switzerland*. PhD thesis, Ecole Polytechnique Fédérale de Lausanne, Lausanne, Switzerland, October 2008.

European Committee for Standardisation. Eurocode 6: Design of masonry structures. European prestandard (pr en 1996-1 :1995), European Committee for Standardisation (CEN), 1995.

P. Fajfar. Capacity spectrum method based on inelastic demand spectra. *Earthquake Engineering and Structural Dynamics*, 28:979–993, 1999.

E. Fehling, J. Stuerz, and A. Emami. Work package 7, deliverable D7.1a Test results on the behaviour of masonry under static (monotonic and cyclic) in plane lateral loads. Technical Report Coll-Ct-2003-500291, Enhanced Safety and Efficient Construction of Masonry Structures in Europe (ESECMaSE), 2007.

FEMA. *HAZUS-MH MR1 Advanced Engineering Building Module*. Federal Emergency Management Agency, Washington, D.C., 2003.

S. Fritsche, D. Fäh, M. Gisler, and D. Giardini. Reconstructing the damage field of the 1855 earthquake in Switzerland: historical investigations on a well-documented event. *Geophysical Journal International*, 166:719–731, 2006.

G. Grünthal, R.M.W. Musson, J. Schwartz, and M. Stucchi. *European Macroseismic Scale 1998*, volume 15. Cahiers du Centre Européen de Géodynamique et de Séismologie, Luxembourg, 1998.

P. Guéguen, C. Michel, and L. Le Corre. A simplified approach for vulnerability assessment in moderate-to-low seismic hazard regions: application to Grenoble (France). *Bulletin of Earthquake Engineering*, 5(3):467–490, August 2007.

S. Hans, C. Boutin, E. Ibraim, and P. Roussillon. In Situ experiments and seismic analysis of existing buildings - Part I: Experimental investigations. *Earthquake Engineering and Structural Dynamics*, 34(12):1513–1529, 2005.

M. Hill and T. Rossetto. Comparison of building damage scales and damage descriptions for use in earthquake loss modelling in europe. *Bulletin of Earthquake Engineering*, 6:335–365, 2008.

E. Kölz and B. Duvernay. Vérification de la sécurité parasismique des bâtiments existants Concept et directives pour l'étape 1. Technical Report Deuxième édition, Office Fédéral des Eaux et de la Géologie, 2005.

K. Konno and T. Ohmachi. Ground motion characteristics estimated from spectral ratio between horizontal and vertical components of microtremor. *Bulletin of the Seismological Society of America*, 88(1):228–241, February 1998.

S. Lagomarsino and S. Giovinazzi. Macroseismic and mechanical models for the vulnerability and damage assessment of current buildings. *Bulletin of Earthquake Engineering*, 4:415–443, 2006.

K. Lang. *Seismic vulnerability of existing buildings*. PhD thesis, ETH Zurich, February 2002.

G. Magenes, P. Morandi, and A. Penna. Work package 7, deliverable D7.1c Test results on the behaviour of masonry under static cyclic in plane lateral loads. Technical Report Coll-Ct-2003-500291, Enhanced Safety and Efficient Construction of Masonry Structures in Europe (ESECMaSE), 2008.

D. E. McNamara and R. P. Buland. Ambient noise levels in the continental united states. *Bulletin of the Seismological Society of America*, 94(4):1517–1527, August 2004.

C. Michel. *Vulnérabilité Sismique de l'échelle du bâtiment à celle de la ville - Apport des techniques expérimentales in situ - Application à Grenoble*. PhD thesis, UJF Grenoble, 2007.

C. Michel. Notre Dame de Valère, Sion. Rapport de test sous vibrations ambiantes. Technical report, Ecole Polytechnique Fédérale de Lausanne, 2009.

C. Michel and M. Oropeza. Post-earthquake survey in L'Aquila (Italy) - Ambient vibration experiment report. Technical Report 9, Ecole Polytechnique Fédérale de Lausanne, Applied Computing and Mechanics Laboratory (EPFL-IMAC), Lausanne, Switzerland, 2009.

C. Michel, P. Lestuzzi, M. Oropeza, and E. Lattion. Seismic Vulnerability of Swiss Masonry buildings: Findings and issues. Technical Report 8, Ecole Polytechnique Fédérale de Lausanne, Applied Computing and Mechanics Laboratory (EPFL-IMAC), 2008.

C. Michel, M. Oropeza, and P. Lestuzzi. Seismic Vulnerability of Existing Masonry Buildings Final Research Report 2009. Technical Report 10, Ecole Polytechnique Fédérale de Lausanne, Applied Computing and Mechanics Laboratory (EPFL-IMAC), Lausanne, Switzerland, 2009a.

C. Michel, B. Zapico, P. Lestuzzi, F. J. Molina, and F. Weber. Quantification of fundamental frequency drop for unreinforced masonry buildings from dynamic tests. *Earthquake Engineering and Structural Dynamics*, submitted, 2009b.

Z. V. Milutinovic and G. S. Trendafiloski. *Risk-UE An advanced approach to earthquake risk scenarios with applications to different european towns. WP4: Vulnerability of current buildings*. European Project, 2003.

M. Oropeza, C. Michel, M. Bigler, and P. Lestuzzi. Improved methodology for estimating main parameters of seismic vulnerability of high-rise unreinforced masonry existing buildings. *submitted to the Bulletin of Earthquake Engineering*, 2009.

A.S. Veletsos and N.M. Newmark. Effect of inelastic behavior on the response of simple systems to earthquake motion. In *2nd World Conference on Earthquake Engineering*, volume 2, pages 895–912, Tokyo, Japan, 1960.

P.D. Welch. The use of Fast Fourier Transform for the estimation of Power Spectra: A method based on time averaging over short, modified periodograms. *I.E.E.E Transactions on Audio and Electroacoustics*, 15(2):70–73, 1967.